Spatiotemporally Multiresolutional Optimization Towards Supply-Demand-Storage Balancing Under PV Prediction Uncertainty

Tomonori Sadamoto, *Student Member, IEEE,* Takayuki Ishizaki, *Member, IEEE,* Masakazu Koike, *Member, IEEE,* Yuzuru Ueda, *Member, IEEE,* Jun-ichi Imura, *Member, IEEE,*

***Abstract*—Large-scale penetration of photovoltaic (PV) power generators and storage batteries is expected in recently constructed power systems. For the realization of smart energy management, we need to make an appropriate day-ahead schedules of power generation and battery charge cycles based on the prediction of demand and PV power generation, which inevitably involves nontrivial prediction errors. With this background, a novel framework is proposed to maintain the balance among the total amounts of power generation, demand, and battery charging power with explicit consideration of the prediction uncertainty assuming that consumer storage batteries are not directly controllable by a supplier. The proposed framework consists of the following three steps: (I) the day-ahead scheduling of the total amount of generation power and battery charging power, (II) the day-ahead scheduling of utility energy consumption requests to individual consumers, which aim to regulate battery charging cycles on the consumer side, and (III) the incentive-based management of the entire power system on the day of interest. In this paper, we especially focus on the day-ahead scheduling problems in Steps (I) and (II) and show that they can be analyzed in a manner originating from spatiotemporal aggregation. Finally, we demonstrate the validity of the proposed framework through numerical verification of the power system management.**

***Index Terms*—Photovoltaic Power Generation, Prediction Uncertainty, Spatiotemporally Multiresolutional Optimization, Supply-Demand-Storage Balancing.**

I. Introduction

A. Background

THE reduction in greenhouse gas emission has been recognized as a long-term goal in the global society as typified by, e.g., the declaration at the G8 Toyako Summit in 2008 [1]. For the realization of such a global goal, the use of renewable energy sources such as photovoltaic (PV) power generation has been gathering attention as an efficient solution technology worldwide. For example, large-scale penetration of PV power generators into the houses of consumers is expected by 2030 in Japan such that the total amount of PV power generation covers approximately 50% of the peak power consumption as well as 10% of the entire energy consumption [2].

It is well known that the existing power system possibly confronts several critical issues due to the large-scale penetration of PV power generators. The major issues include the deviation from an allowable frequency range, which can be caused when the total amount of power generation including PV power generation exceeds the total amount of power consumption by consumers. One approach to handle this issue is to discard the surplus PV power generation; however, this is not necessarily efficient from the viewpoint of smart energy management. As another approach, the installation of storage batteries has the potential to use the surplus effectively. Note that it is desirable to introduce storage batteries to individual consumers with PV power generators in order to prevent reverse power flow into the grid. In the following, we use the term "demand" to represent the amount of power obtained by subtracting the amount of PV power generation from the amount of power consumption by consumers.

In this paper, we aim to develop a framework to maintain the balance among the total amounts of power generation, demand, and battery charging power in a power system involving a large number of PV power generators and storage batteries. We assume that every consumer has a PV power generator and storage battery, whereas the supplier side has no PV power generators and storage batteries. Throughout this paper, we refer to this type of supply-demand balance as "supply-demand-storage balance." In this framework, we determine the day-ahead schedules of power generation and battery charge cycles according to the prediction of demand to manage the power system efficiently.

In detail, we first consider the case where demand prediction can be exactly performed, i.e., no prediction uncertainty exists. By definition, the total amount of demand should be equal to the sum of the total amounts of power generation and battery discharging power, which originate from the supply and consumer sides, respectively. This equality implies that a supplier can automatically obtain the scheduling of the total number of battery charge cycles from that of the total power generation as long as the demand prediction is ideally performed. However, even in such an ideal situation, the storage batteries are not necessarily charged in compliance with the scheduling of the total number of battery charge cycles, as expected on the supplier side, because the total battery charge cycles in the consumer side cannot be controlled

Manuscript received XXXX, 2014; revised XXXX, 2014.

T. Sadamoto, T. Ishizaki, M. Koike and J. Imura are with Graduate School of Information Science and Engineering, Tokyo Institute of Technology; 2-12-1, Ookayama, Meguro, Tokyo, 152-8552, Japan. e-mail: {sadamoto, ishizaki, koike, imura}@cyb.mei.titech.ac.jp.

Y. Ueda is with Department of Electrical Engineering, Tokyo University of Science; 6-3-1 Niijuku, Katsushika-ku, Tokyo, 125-8585, Japan. e-mail: ueda@ee.kagu.tus.ac.jp.

All authors are with CREST, Japan Science and Technology Agency; Honcho, Kawaguchi, Saitama, Japan.

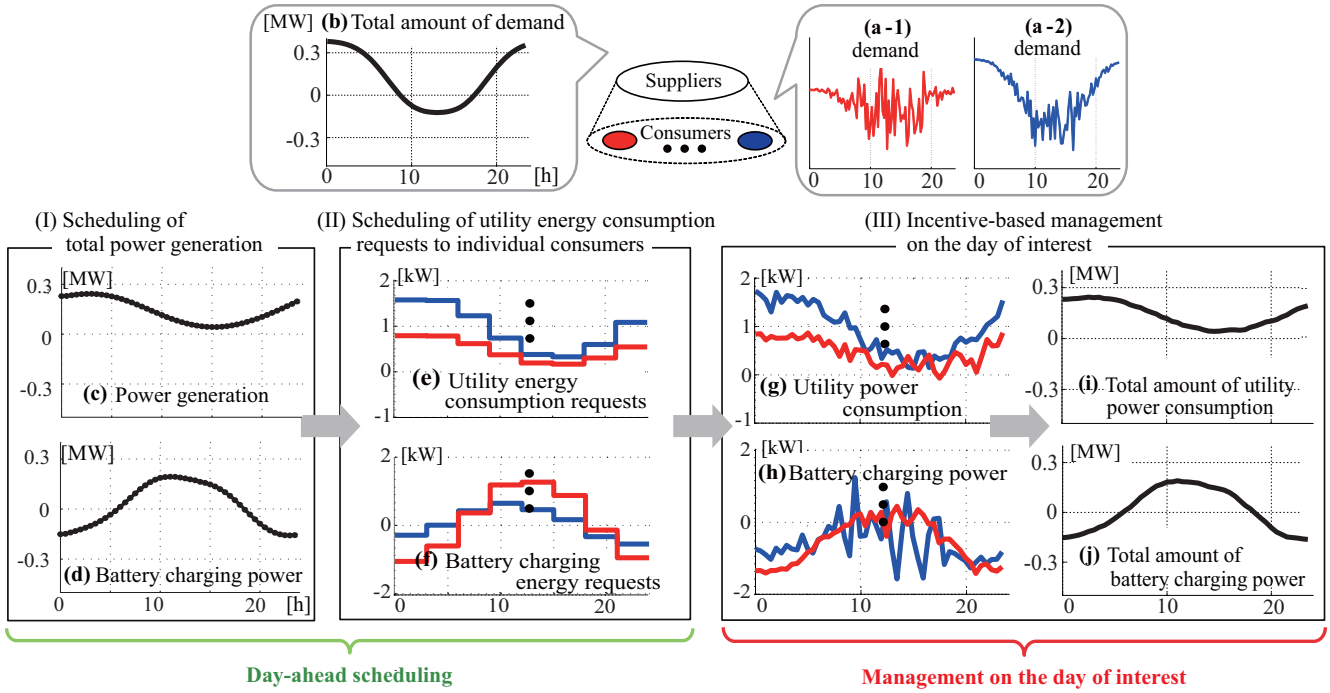

Fig. 1. Proposed framework for supply-demand-storage balance. (A1)

directly by the supplier. In addition to this difficulty, it is obvious that exact demand prediction is not realistic owing to the steep fluctuations in PV power generation [3], [4], [5], and the idiosyncratic behavior of individual consumers.

With this background, we propose a framework to maintain the supply-demand-storage balance, in which a load dispatching center provides some requests to individual consumers, which aim to regulate battery charge cycles on the consumer side. In our framework, it is crucial to determine the day-ahead schedules of power generation as well as the requests to consumers while explicitly considering the uncertainty of demand prediction and the idiosyncratic behavior of individual consumers.

B. Proposed Framework

In this subsection, we explain the framework needed to realize the supply-demand-storage balance with the background in Section I-A. In detail, we first consider the two-layered power system depicted at the top of Fig. 1. Our framework consists of the following three steps: (I) the day-ahead scheduling of the total amount of power generation, which subserviently yields the scheduling of the total number of battery charge cycles, (II) the day-ahead scheduling of utility energy consumption requests to individual consumers, which aim to regulate battery charge cycles on the consumer side, and (III) the incentive-based management of the entire power system on the day of interest. In what follows, we formulate these steps in a discrete-time setting, where the term "utility power" is used to represent the amount of power at a power-receiving point of consumer's home, and its integral is referred to as "utility energy."

In Step (I), the day-ahead schedules of total power generation and battery charge cycles are determined on the basis of the day-ahead prediction of the total amount of demand. Note that the total demand, depicted in Fig. 1(b), is given by the spatial aggregation of the demand of individual consumers, depicted in Figs. 1(a-1) and (a-2). Thus, we can expect that the uncertainty of the spatially aggregated demand prediction consisting of PV power generation and power consumption becomes smaller than that with respect to each consumer. Owing to such an effect, known as the smoothing effect [6], [7], the resulting power generation schedule and battery charge cycles, depicted in Figs. 1(c) and (d), respectively, can be determined in a manner that is robust against the prediction uncertainty.

In Section II-B, we will mathematically formulate this scheduling problem of total power generation, denoted as Problem 1, on the basis of the premise that the predicted demand is given as a stochastic variable. It should be noted that the scheduling of the total number of battery charge cycles is not required in a conventional power system, where PV power generators and storage batteries have not sufficiently penetrated. Because the schedule of total power generation in Fig. 1(c) can be regarded as the total power consumption (or total load) in a conventional power system, we can subsequently perform the detailed scheduling of individual generators after determining it. For example, unit commitment and economic dispatch control can be applied with a time step that is commensurate with the economic dispatch process in the time range of interest, e.g., from 1/6 [h] to 1 [h].

In Step (II), a load dispatching center determines the schedule of utility power consumption requests to individual consumers on the basis of the prediction of PV power generation and power consumption of individual consumers as well as the resulting power generation schedule in Step (I). This aims to regulate battery charge cycles on the consumer side. Note that the requests should be reasonable in the sense that individual consumers can naturally follow them,

namely, a degree of freedom with respect to the utility power consumption should be reasonably ensured for each consumer. In view of this, we consider determining these requests as *utility energy consumption requests*, i.e., requests of the utility power consumption averaged over a relatively long period, as depicted in Fig. 1(e), which subserviently yield the battery charging energy requests in Fig. 1(f). Such requests indeed involve a degree of freedom with respect to the utility power consumption because individual consumers can consume their utility power within the limits of an energy regulation. Note that a load dispatching center regulates only the amount of temporally aggregated utility power consumption. The use of temporally aggregated demand prediction, having good compatibility with the request of utility energy consumption, allows us to reduce the prediction uncertainty, similar to the aforementioned spatial aggregation.

In Section II-C, we will formulate this scheduling problem, denoted as Problem 2, on the basis of the premise that a power generation schedule is determined in Step (I). Furthermore, we will formulate an optimization problem originating from spatiotemporal aggregation, denoted as Problem 3, in Section III to analyze the degree of prediction uncertainty relaxation via spatial and temporal aggregation in Steps (I) and (II). This formulation enables us to perform a robustness analysis of the power generation and request scheduling in a unified manner. Moreover, it enables a generalization of our framework to multilayered power systems involving several electrical substations.

In Step (III), we manage the entire power system according to the resulting schedules of total power generation in Step (I) and utility energy consumption requests to individual consumers in Step (II). In detail, we suppose that the utility power consumption of each consumer, depicted in Fig. 1(g), results in compliance with the corresponding utility energy consumption request in each time interval, depicted in Fig. 1(e). In the same manner, the battery charge cycles of each consumer result in Fig. 1(h). The utility power consumption and battery charge cycles of each consumer yield their totals for all consumers in Figs. 1(i) and (j), which are expected to be close to the scheduled ones depicted in Figs. 1(c) and (d). Such an expectation would be reasonable if the behavior of each consumer is sufficiently disperse. The closeness between the total utility power consumption and the schedule of total power generation implies that only a small regulating capacity is required to compensate for their difference, i.e., to maintain the supply-demand-storage balance.

In general, consumers do not necessarily follow the utility energy consumption requests from the load dispatching center. A possible way to make consumers follow the requests would be to provide an incentive to consumers or to implement a billing system in which power bills are calculated on the basis of the deviation from the requests. However, the determination of a rigorous incentive or billing system is not necessarily easy because it requires a detailed consumer model that captures the behavior with regard to incentives or power bills, which would require vast experiments with real consumers to construct. On the other hand, our framework has a potential to be adapted to many types of incentive or billing systems. In view of this, we qualitatively investigate via the numerical verification in Section IV what types of them make the utility energy consumption requests reasonable in the sense that the total amount of actual utility power consumption is made closer to the optimal schedule of total power generation.

In terms of a smart grid, we suppose that the prediction of PV power generation and power consumption as well as the information on storage batteries, such as the inverter capacity and initial battery energy, are available for scheduling of the total power generation and battery charge cycles. In addition, we suppose that a home energy management system performs an optimization with respect to incentives or power bills determined on the basis of the deviation from utility energy consumption requests.

C. Related Work

In this paper, we deal with the uncertainty of demand prediction in a stochastic manner and formulate the day-ahead scheduling problems in terms of chance constrained optimization. In fact, a number of studies on stochastic optimization can be found in the literature. For example, [8] addresses a chance constrained optimization problem to find the optimal power flow, and [9] and [10] address problems of stochastic unit commitment. In these papers, the uncertainty of wind power generation is expressed as a stochastic variable. However, the problem formulation in the first paper does not consider the use of storage batteries, whereas the formulations in the second and third papers only consider the case in which storage batteries can be directly controllable from the supplier side. By assuming directly controllable storage batteries, [11] similarly develops a method of model predictive control for battery charge cycles with the stochastic modeling of uncertain renewable energy sources. Note that our problem formulation is different because it is based on the premise that battery charging cycles on the consumer side are not directly controllable from the supplier side.

On the other hand, several studies on the control of the aggregated amount of consumer-side quantities such as power consumption can also be found in the literature. For example, [12] addresses a demand control problem in which the on–off switching of deferrable appliances is applied to the peak shift in the total demand. In a similar work, [13] analyzes the supply-demand balance with regard to the total amount of deferrable demand as a type of an energy storage. The concept in both papers is based on utilizing the aggregated amount of deferrable (flexible) demand, which is assumed to be fully controllable by the supplier side (or an organizer). This clearly contrasts with our concept based on the idea that the small dispersion of consumer-side quantities is imperceptible to the supplier side owing to spatiotemporal aggregation, exemplified as a smoothing effect. From this viewpoint, we propose a method to determine low temporal resolution requests to individual consumers assuming that the storage batteries in the consumer side are not directly controllable, which can ensure a degree of freedom with respect to utility power consumption and battery charge cycles.

In [14], the authors have developed basic mathematical tools for solving and analyzing the chance constrained optimization

problem based on spatial and temporal aggregation. However, their practical interpretation and relation to the supply-demand-storage balancing are not thoroughly discussed. In contrast, this paper aims to construct a practical framework to maintain the supply-demand-storage balance while providing a detailed implementation procedure. Moreover, we provide a unified problem formulation originating from spatiotemporal aggregation.

D. Organization

The reminder of this paper is structured as follows. In Section II-A, we first introduce a mathematical model of the temporal variation in battery charging energy and then formulate the scheduling problems for the total power generation and utility energy consumption requests in Sections II-B and II-C, respectively. In Section III-A, we formulate a unified optimization problem originating from spatiotemporal aggregation. Then, we theoretically show the positive effect of spatiotemporal aggregation for robustness against the prediction uncertainty of demand in Section III-B. Section IV is devoted to a demonstration of the proposed framework via a numerical simulation. Finally, concluding remarks are provided in Section V.

II. Problem Formulation

A. Mathematical Model

First, we introduce a mathematical model of the power systems discussed in this paper. Let

$$\mathbb{T} := \{0, \dots, T-1\} \tag{1}$$

be the time horizon of interest, and suppose that the time length T satisfies

$$T = 24/\kappa \tag{2}$$

where κ [h] is a size of the time step. Furthermore, let n be the number of consumers with PV power generators, and denote the amount of power consumption and PV power generation at time t by $p_t \in \mathbb{R}^n$ and $p'_t \in \mathbb{R}^n$, respectively. Then, we define the *net* amount of demand at time t by

$$d_t := p_t - p'_t \in \mathbb{R}^n, \tag{3}$$

which may have negative elements. Furthermore, assuming that every consumer has a storage battery, we model the temporal variation in the battery energy by

$$x_{t+1} = x_t + \kappa(v_t - d_t), \quad t \in \mathbb{T} \tag{4}$$

where $x_t \in \mathbb{R}^n$ and $v_t \in \mathbb{R}^n$ denote the battery energy and the utility power consumption of consumers at time t, respectively. Note that κ satisfies (2), and the initial battery energy x_0 is supposed to be a fixed constant. The difference equation in (4) represents the energy originating from the deviation between the utility power consumption and the demand to be charged into each storage battery.

B. Scheduling Problem of Total Power Generation

In this subsection, we formulate a scheduling problem for the total amount of power generation while explicitly considering the prediction uncertainty of demand. This problem is to be solved at Step (I) in our framework mentioned in Section I-B, and it corresponds to Fig. 1 (I).

We model d_t in (3) as a stochastic variable. In particular, we consider the predicted demand as a normally distributed variable, namely

$$\mathbf{d} = [\mathbf{d}_t]_{t\in\mathbb{T}} \sim \mathcal{N}(d, \Sigma), \quad d := [d_t]_{t\in\mathbb{T}} \in \mathbb{R}^{nT}. \tag{5}$$

Note that the mean value of $\mathbf{d}$ is given to comply with d_t, and its covariance matrix is given by the symmetric positive semidefinite matrix $\Sigma \in \mathbb{R}^{nT\times nT}$, which reflects the uncertainty of demand prediction. In this paper, the magnitude of Σ is supposed to be large in the sense of its norm. In the following, we express stochastic variables in boldface, e.g., $\mathbf{d}$.

For the predicted demand $\mathbf{d}$ in (5), the total amount of predicted demand is given by

$$\mathbf{D} := [\mathbf{D}_t]_{t\in\mathbb{T}} \in \mathbb{R}^T, \quad \mathbf{D}_t := \mathbf{1}_n^\mathsf{T}\mathbf{d}_t, \tag{6}$$

which can be regarded as the spatial aggregation of each $\mathbf{d}_t$. Note that the temporal sequences of $\mathbf{d}_t$ and $\mathbf{D}_t$ correspond to the plots in Figs. 1(a) and (b), respectively. For compatibility with (4), the temporal variation in the total amount of battery energy can be expressed as

$$\mathbf{X}_{t+1} = \mathbf{X}_t + \kappa(V_t - \mathbf{D}_t), \quad t \in \mathbb{T} \tag{7}$$

where $\mathbf{X}_t \in \mathbb{R}$ denotes the total battery energy, whose initial value is given as $\mathbf{X}_0 = \mathbf{1}_n^\mathsf{T}x_0$, and $V_t \in \mathbb{R}$ denotes the total amount of power generation, whose temporal sequence is to be determined. Note that the size of a time step κ should be small enough to obtain an appropriate schedule valid for real-time balancing. In particular, κ should be commensurate with the economic dispatch process of interest in the range, e.g., from 1/6 [h] to 1 [h]. Furthermore, $\mathbf{X}_t$ should be a stochastic variable because $\mathbf{D}_t$ is.

Next, we give a cost function that evaluates the fuel cost of the generators and the deterioration of the storage batteries due to discharging. In the rest of this paper, similar to $\mathbf{D}$ in (6), we use the following notation:

$$V := [V_t]_{t\in\mathbb{T}} \in \mathbb{R}^T, \quad \mathbf{X} := [\mathbf{X}_t]_{t\in\mathbb{T}} \in \mathbb{R}^T.$$

Furthermore, the total amount of battery charging power is denoted as

$$\Delta\mathbf{X} := [\Delta\mathbf{X}_t]_{t\in\mathbb{T}} \in \mathbb{R}^T, \quad \Delta\mathbf{X}_t := \frac{1}{\kappa}\left(\mathbf{X}_{t+1} - \mathbf{X}_t\right). \tag{8}$$

In this notation, we express the cost function as (A3)

$$J(V; \Delta\mathbf{X}) := \sum_{t=0}^{T-1} \left\{ f(V_t) + \mathbb{E}\left[g(\Delta\mathbf{X}_t)\right] \right\} \tag{9}$$

where $f(\cdot)$ and $g(\cdot)$ are convex functions that evaluate the fuel cost of the generators and the deterioration cost of the storage batteries caused by discharging, respectively. Their specification will be described in Section IV devoted to a numerical verification. In this cost function, for simplicity, the

total fuel cost of multiple generators and the total deterioration cost of multiple storage batteries are approximately evaluated as those of average generators and storage batteries, although it is possible to enhance the evaluation to account for the varieties of the generators and storage batteries.

We define a constraint condition that represents some physical limitation. Taking into account the stochastic aspect of $\mathbf{X}$, the constraint condition is given as a set of chance constraints [15], [16], [17]. To this end, we use the following notation:

$$\Pi(\mathbf{x};\mathcal{I},\epsilon) := \left(\Pr(\mathbf{x} \geq \underline{\mathcal{I}}) \geq 1-\epsilon\right) \wedge \left(\Pr(\mathbf{x} \leq \overline{\mathcal{I}}) \geq 1-\epsilon\right)$$

where $\mathcal{I} = [\underline{\mathcal{I}}, \overline{\mathcal{I}}]$ and $\epsilon \in (0,1)$ denote an interval and a violation rate, respectively. This constraint of Π implies that the probabilities of both $\mathbf{x} \geq \underline{\mathcal{I}}$ and $\mathbf{x} \leq \overline{\mathcal{I}}$ must be equal or greater than $1-\epsilon$. Then, we impose a set of chance constraints on $\mathbf{X}$ as

$$\begin{cases} \Pi(\mathbf{X}_t;\mathcal{I}_1,\epsilon_1), \quad \Pi(\Delta\mathbf{X}_t;\mathcal{I}_2,\epsilon_2), \quad \forall t \in \mathbb{T} \\ \Pi(\mathbf{X}_T;\mathcal{I}_3,\epsilon_3). \end{cases} \tag{10}$$

The constraints in the first line restrict the total amount of battery energy and battery charging power to their maximum and minimum limits, described by the intervals $\mathcal{I}_1$ and $\mathcal{I}_2$. The constraint in the second line is given so that the total battery energy $\mathbf{X}_T$ at the terminal time $t = T$ falls within the desired interval $\mathcal{I}_3 \subseteq \mathcal{I}_1$ for the sustainable use of the storage batteries. In addition, we impose a deterministic constraint on V as

$$V_t \in \mathcal{I}_4, \quad \forall t \in \mathbb{T}. \tag{11}$$

In this notation, the scheduling problem for the total power generation is formulated as follows:

Problem 1: Let a predicted demand $\mathbf{d}$ in (5) be given. For the system in (7) with $\mathbf{D}$ in (6), define the cost function as in (9). Then, find

$$V^* := \underset{V \in \mathbb{R}^T}{\operatorname{argmin}}\, J(V;\Delta\mathbf{X}) \tag{12}$$

subject to (7), (10) and (11).

In Problem 1, we formulate a problem to find the optimal schedule of total power generation, denoted by $V^* \in \mathbb{R}^T$. Once V^* is found, we can subserviently obtain the optimal schedule of the total number of battery charge cycles with (7). These optimal schedules of total generation power and battery charge cycles correspond to the plots in Figs. 1(c) and (d), respectively. Even though constraints on network and security are not considered in this problem, they can be involved in unit commitment and economic dispatch control, applied to the resulting schedule of total generation power.

For the development of a reliable framework to maintain the supply-demand-storage balance, it is desired that the optimal schedules are robust against the uncertainty of demand prediction. Note that the prediction uncertainty is expressed as the covariance matrix Σ of $\mathbf{d}$ in (5). In view of this, we can say that the scheduling problem is robust against the prediction uncertainty if the sensitivity of V^* in (12) to the magnitude of Σ is low enough. Such a robustness analysis will be performed in Section III-B.

C. Scheduling Problem of Utility Energy Consumption Requests

In this subsection, we formulate a scheduling problem for utility energy consumption requests to individual consumers. This problem is to be solved at Step (II) in our framework mentioned in Section I-B, and it corresponds to Fig. 1 (II). We first introduce a *sparse* time scale $\hat{\mathbb{T}}$ as

$$\hat{\mathbb{T}} := \{0, \ldots, \hat{T}-1\}. \tag{13}$$

For this sparse time scale, we assume that there exists a natural number τ, which represents the degree of *temporal resolution*, such that

$$\tau\hat{T} = T. \tag{14}$$

In this sparse time scale, the size of a time step is given by

$$\hat{\kappa} := \tau\kappa, \tag{15}$$

where κ satisfies (2).

In the following, we give a formulation to determine utility energy consumption requests, which are provided from a load dispatching center to consumers. The requests aim to regulate the amount of utility energy consumption, i.e., the utility power averaged over the period given by τ, which regulates the battery charging energy of each consumer subserviently.

Assuming that the optimal schedule of total power generation, denoted by V^* in (12), is determined in advance, we consider $\hat{v}_{\hat{t}} \in \mathbb{R}^n$ denoting the utility energy consumption requests to all consumers at time $\hat{t}$. We derive the difference equation representing the temporal variation in battery energy at the sparse time scale. The corresponding amount of predicted demand $\mathbf{d}$ in (5) is given by

$$\hat{\mathbf{d}} := [\hat{\mathbf{d}}_{\hat{t}}]_{\hat{t}\in\hat{\mathbb{T}}} \in \mathbb{R}^{n\hat{T}}, \quad \hat{\mathbf{d}}_{\hat{t}} := \frac{1}{\tau}(\mathbf{d}_{\tau\hat{t}} + \cdots + \mathbf{d}_{\tau(\hat{t}+1)-1}), \tag{16}$$

which can be regarded as the temporal aggregation of $\mathbf{d}$. In this notation, the temporal variation in the battery energy can be expressed as

$$\hat{\mathbf{x}}_{\hat{t}+1} = \hat{\mathbf{x}}_{\hat{t}} + \hat{\kappa}(\hat{v}_{\hat{t}} - \hat{\mathbf{d}}_{\hat{t}}), \quad \hat{t} \in \hat{\mathbb{T}} \tag{17}$$

where $\hat{\mathbf{x}}_{\hat{t}} \in \mathbb{R}^n$ denotes the battery energy of all consumers at time $\hat{t}$, whose initial value is given as $\hat{\mathbf{x}}_0 = x_0$.

Next, similar to (10), we give a set of chance constraints on $\hat{\mathbf{x}} := [\hat{\mathbf{x}}_{\hat{t}}]_{\hat{t}\in\hat{\mathbb{T}}} \in \mathbb{R}^{n\hat{T}}$ as

$$\begin{cases} \Pi(\hat{\mathbf{x}}_{\hat{t}};\hat{\mathcal{I}}_1,\hat{\epsilon}_1), \quad \Pi(\Delta\hat{\mathbf{x}}_{\hat{t}};\hat{\mathcal{I}}_2,\hat{\epsilon}_2), \quad \forall \hat{t} \in \hat{\mathbb{T}} \\ \Pi(\hat{\mathbf{x}}_{\hat{T}};\hat{\mathcal{I}}_3,\hat{\epsilon}_3) \end{cases} \tag{18}$$

where the average charging power is denoted by

$$\Delta\hat{\mathbf{x}} := [\Delta\hat{\mathbf{x}}_{\hat{t}}]_{\hat{t}\in\hat{\mathbb{T}}} \in \mathbb{R}^{n\hat{T}}, \quad \Delta\hat{\mathbf{x}}_{\hat{t}} := \frac{1}{\hat{\kappa}}\left(\hat{\mathbf{x}}_{\hat{t}+1} - \hat{\mathbf{x}}_{\hat{t}}\right). \tag{19}$$

In addition, similar to (11), we impose deterministic inequality constraints on $\hat{v}_{\hat{t}}$ as

$$\hat{v}_{\hat{t}} \in \hat{\mathcal{I}}_4, \quad \forall \hat{t} \in \hat{\mathbb{T}}. \tag{20}$$

Furthermore, we define an objective function that evaluates the degradation of economic efficiency. In particular, for the temporal sequence of utility energy consumption requests

denoted by $\hat{v} := [\hat{v}_{\hat{t}}]_{\hat{t}\in\hat{\mathbb{T}}} \in \mathbb{R}^{n\hat{T}}$, we define the objective function as

$$\hat{J}(\hat{v}) := \left\| V^* - [\mathbf{1}_\tau \mathbf{1}_n^\mathsf{T} \hat{v}_{\hat{t}}]_{\hat{t}\in\hat{\mathbb{T}}} \right\|^2. \tag{21}$$

The meaning of $\hat{J}$ in (21) can be explained as follows: First, we see that $[\mathbf{1}_n^\mathsf{T}\hat{v}_{\hat{t}}]_{\hat{t}\in\hat{\mathbb{T}}} \in \mathbb{R}^{\hat{T}}$ represents the temporal sequence of the total number of utility energy consumption requests for all consumers. Furthermore, its temporal interpolation based on the zero-order hold is given by $[\mathbf{1}_\tau \mathbf{1}_n^\mathsf{T}\hat{v}_{\hat{t}}]_{\hat{t}\in\hat{\mathbb{T}}} \in \mathbb{R}^{T}$, which corresponds to the supposition that every consumer tries to follow the utility energy consumption request as *constant utility power consumption* in each time interval. Under this supposition, we evaluate the discrepancy between the optimal schedule of total power generation and the total amount of utility energy consumption requests. Note that this discrepancy can be regarded as a degradation in economic efficiency because V^* is determined to improve economic efficiency with respect to the total power generation and battery charge cycles.

In this notation, the scheduling problem for utility energy consumption requests is formulated as follows:

Problem 2: Let the predicted demand $\mathbf{d}$ in (5) and the optimal power generation schedule V^* in (12) be given. For the system in (17) with $\hat{\mathbf{d}}$ in (16), define the objective function as in (21). Then, find

$$\hat{v}^* := \operatorname*{argmin}_{\hat{v}\in\mathbb{R}^{n\hat{T}}} \hat{J}(\hat{v}) \tag{22}$$

subject to (17), (18) and (20).

In the above formulation, the parameter τ represents a degree of freedom that allows consumers to idiosyncratically consume utility power within the limits of an energy regulation. This optimal schedule of utility energy consumption requests corresponds to the plot in Fig. 1(e), where the temporal interpolation based on the zero-order hold is applied to draw. Furthermore, the scheduled requests subserviently yield those of the battery charging energy in Fig. 1 (f).

III. Analysis Based on Spatiotemporal Aggregation

A. A Unified Formulation of the Two Scheduling Problems

In this section, we give a robustness analysis of Problems 1 and 2 in Sections II-B and II-C. To analyze the two optimization problems in a unified manner, we introduce a general formulation originating from spatiotemporal aggregation.

We assume that there exist natural numbers ν and $\hat{n}$ such that

$$\nu\hat{n} = n. \tag{23}$$

For the the predicted demand $\mathbf{d}$ in (5), as a generalization of (6) and (16), we define a spatiotemporally aggregated predicted demand by

$$\hat{\mathbf{D}} = [\hat{\mathbf{D}}_{\hat{t}}]_{\hat{t}\in\hat{\mathbb{T}}} \sim \mathcal{N}(\hat{D}, \hat{\Sigma}), \quad \begin{cases} \hat{D} := Wd \\ \hat{\Sigma} := W\Sigma W^\mathsf{T} \end{cases} \tag{24}$$

where the spatiotemporal aggregation matrix is defined by

$$W := \frac{1}{\tau}\mathrm{diag}_{\hat{T}}\left(\left[\mathrm{diag}_{\hat{n}}(\mathbf{1}_\nu^\mathsf{T}), \ldots, \mathrm{diag}_{\hat{n}}(\mathbf{1}_\nu^\mathsf{T})\right]\right) \in \mathbb{R}^{\hat{n}\hat{T}\times nT}. \tag{25}$$

Furthermore, as a unified form of (7) and (17), we express an $\hat{n}$-dimensional stochastic system as

$$\hat{\mathbf{X}}_{\hat{t}+1} = \hat{\mathbf{X}}_{\hat{t}} + \hat{\kappa}(\hat{V}_{\hat{t}} - \hat{\mathbf{D}}_{\hat{t}}), \quad \hat{t} \in \hat{\mathbb{T}} \tag{26}$$

where the initial value is given as $\hat{\mathbf{X}}_0 = \mathrm{diag}_{\hat{n}}(\mathbf{1}_\nu^\mathsf{T})x_0$, and

$$\hat{V} := [\hat{V}_{\hat{t}}]_{\hat{t}\in\hat{\mathbb{T}}} \in \mathbb{R}^{\hat{n}\hat{T}}, \quad \hat{\mathbf{X}} := [\hat{\mathbf{X}}_{\hat{t}}]_{\hat{t}\in\hat{\mathbb{T}}} \in \mathbb{R}^{\hat{n}\hat{T}}$$

represent the spatiotemporal aggregation of the corresponding variables. Indeed, if $\tau = 1$ and $\nu = n$, then (24) and (26) coincide with (6) and (7), and if $\nu = 1$, they coincide with (16) and (17).

In a similar manner, for compatibility with (9) and (21), we express a cost function as

$$J(\hat{V}; \Delta\hat{\mathbf{X}}) := F(\hat{V}) + \mathbb{E}[G(\Delta\hat{\mathbf{X}})], \tag{27}$$

where $F(\cdot)$ and $G(\cdot)$ are the corresponding convex functions, and define

$$\Delta\hat{\mathbf{X}} := [\Delta\hat{\mathbf{X}}_{\hat{t}}]_{\hat{t}\in\hat{\mathbb{T}}}, \quad \Delta\hat{\mathbf{X}}_{\hat{t}} := \frac{1}{\hat{\kappa}}\left(\hat{\mathbf{X}}_{\hat{t}+1} - \hat{\mathbf{X}}_{\hat{t}}\right), \tag{28}$$

being compatible with (8) and (19). Moreover, the set of chance constraints can be expressed as

$$\Pr\left(a_i \begin{bmatrix} \hat{\mathbf{X}} \\ \hat{V} \\ \hat{\mathbf{D}} \end{bmatrix} \le b_i\right) \ge 1 - \delta_i, \quad \forall i \in \{1, \ldots, n_\mathrm{c}\} \tag{29}$$

where n_c represents the number of constraints, $\delta_i \in (0, 1)$ represents the rate of violation, and $a_i \in \mathbb{R}^{1\times 3\hat{n}\hat{T}}$ and $b_i \in \mathbb{R}$ are coefficients compatible with (10) and (18). Finally, the deterministic inequality constraints can be expressed as

$$A\hat{V} \le b \tag{30}$$

where $A \in \mathbb{R}^{m\times\hat{n}\hat{T}}$ and $b \in \mathbb{R}^m$ are coefficients compatible with (11) and (20). In this notation, we consider the following chance constrained optimization problem:

Problem 3: Let the predicted demand $\mathbf{d}$ in (5) be given. For the system in (26) with $\hat{\mathbf{D}}$ in (24), define the cost function as in (27). Then, find

$$\hat{V}^* := \operatorname*{argmin}_{\hat{V}\in\mathbb{R}^{\hat{n}\hat{T}}} J(\hat{V}; \Delta\hat{\mathbf{X}}) \tag{31}$$

subject to (26), (29) and (30).

Problem 3 can handle Problems 1 and 2, solved at Steps (I) and (II) in Section I-B, in a unified manner. In this formulation, W in (25) serves as the spatiotemporal aggregation. Furthermore, the parameters ν and τ represent degrees of *spatial resolution* and *temporal resolution*.

Note that, owing to this generalization, we can deal with the problem of a hierarchical determination of the requests to consumers through intermediate determination of those to several electrical substations. To see this more clearly, we consider a power system composed of three layers. Our objective here is to determine the requests to individual consumers in the lowest layer via the determination of requests to several areas, i.e., clusters of consumers, in the middle layer. To this end, we first find the optimal schedule of the total power generation V^* by solving Problem 1. Then, to determine the

optimal intermediate requests $\hat{V}^*$ to $\hat{n}$ areas, each of which includes ν consumers, we solve Problem 3 with $\hat{\mathbf{D}}$, $\hat{V}$ and $\hat{\mathbf{X}}$, which denote the spatiotemporally aggregated demand, the intermediate requests of utility energy consumption, and the compatible battery energy, respectively. Finally, we find the requests to individual consumers as the solution of Problem 2 where we replace V^* with $\hat{V}^*$.

B. Analysis of Robustness against Prediction Uncertainty

In this subsection, we investigate the positive effects of spatiotemporal aggregation on the feasibility of Problem 3. First, we describe the following lemma to equivalently translate Problem 3 into a deterministic convex optimization problem as follows:

Proposition 1: Consider Problem 3. Let $\hat{D}_{\hat{t}}$ denote the $\hat{t}$th element of $\hat{D}$ in (24), and define an $\hat{n}$-dimensional model by

$$\hat{X}_{\hat{t}+1} = \hat{X}_{\hat{t}} + \hat{\kappa}(\hat{V}_{\hat{t}} - \hat{D}_{\hat{t}}), \quad \hat{t} \in \hat{\mathbb{T}} \tag{32}$$

where $\hat{X}_0 = \mathrm{diag}(\mathbf{1}_\nu^\mathsf{T})x_0$. Furthermore, define

$$\begin{aligned} \hat{V} &:= [\hat{V}_{\hat{t}}]_{\hat{t}\in\hat{\mathbb{T}}} \in \mathbb{R}^{\hat{n}\hat{T}}, \quad \Delta\hat{X} := [\Delta\hat{X}_{\hat{t}}]_{\hat{t}\in\hat{\mathbb{T}}} \in \mathbb{R}^{\hat{n}\hat{T}}, \\ \hat{X} &:= [\hat{X}_{\hat{t}}]_{\hat{t}\in\hat{\mathbb{T}}} \in \mathbb{R}^{\hat{n}\hat{T}} \end{aligned} \tag{33}$$

where

$$\Delta\hat{X}_{\hat{t}} := \frac{1}{\hat{\kappa}}(\hat{X}_{\hat{t}+1} - \hat{X}_{\hat{t}}).$$

Then, for the convex function defined by (A3)

$$\overline{G}(x) := \int_{-\infty}^{\infty} \frac{G(\xi)}{\sqrt{(2\pi)^{\hat{n}\hat{T}}|\hat{\Sigma}|^\dagger}} e^{-\frac{1}{2}(\xi-x)^\mathsf{T}\hat{\Sigma}^\dagger(\xi-x)} d\xi \tag{34}$$

where $|\hat{\Sigma}|^\dagger$ and $\hat{\Sigma}^\dagger$ denote the pseudo-determinant and the Moore-Penrose pseudo-inverse of $\hat{\Sigma}$, respectively [18], $\hat{V}^*$ in (31) coincides with

$$\hat{V}^* = \underset{\hat{V}\in\mathbb{R}^{\hat{n}\hat{T}}}{\mathrm{argmin}} \Big(F(\hat{V}) + \overline{G}(\Delta\hat{X}) \Big) \tag{35}$$

subject to (30), (32) and

$$a_i \begin{bmatrix} \hat{X} \\ \hat{V} \\ \hat{D} \end{bmatrix} < b_i - s_i(\hat{\Sigma}, \delta_i), \quad \forall i \in \{1, \dots, n_\mathrm{c}\} \tag{36}$$

where

$$s_i(\hat{\Sigma}, \delta_i) := \sqrt{2c_i\hat{\Sigma}c_i^\mathsf{T}}\ \mathrm{erf}^{-1}(1-2\delta_i) \tag{37}$$

with

$$c_i := a_i \begin{bmatrix} \hat{\kappa}M \\ 0 \\ I_{\hat{n}\hat{T}} \end{bmatrix} \in \mathbb{R}^{1\times\hat{n}\hat{T}}, \ M := \begin{bmatrix} 0 & 0 & \cdots & 0 \\ I_{\hat{n}} & 0 & \cdots & 0 \\ \vdots & \ddots & \ddots & \vdots \\ I_{\hat{n}} & \cdots & I_{\hat{n}} & 0 \end{bmatrix} \in \mathbb{R}^{\hat{n}\hat{T}\times\hat{n}\hat{T}}.$$

Proof: First, from (26) with (28), we notice that $\Delta\hat{\mathbf{X}} \sim \mathcal{N}(\Delta\hat{X}, \hat{\Sigma})$, where its mean is denoted as $\Delta\hat{X}$. Thus, it follows that (A3)

$$\mathbb{E}[G(\Delta\hat{\mathbf{X}})] = \overline{G}(\Delta X).$$

In the following, we show the convexity of $\overline{G}(\cdot)$. Note that the convexity of $G(\cdot)$ implies that

$$G(x_\alpha) \le \alpha G(x) + (1-\alpha)G(x'), \quad x_\alpha := \alpha x + (1-\alpha)x'$$

for all $x, x' \in \mathbb{R}^{\hat{n}\hat{T}}$ and $\alpha \in [0,1]$. Thus, letting $\zeta := \xi - x$, we have

$$\begin{aligned} \overline{G}(x_\alpha) &= \int_{-\infty}^{\infty} \frac{G(\zeta+x_\alpha)}{\sqrt{(2\pi)^{\hat{n}\hat{T}}|\hat{\Sigma}|^\dagger}} e^{-\frac{1}{2}\zeta^\mathsf{T}\hat{\Sigma}^\dagger\zeta} d\zeta \\ &\le \int_{-\infty}^{\infty} \frac{\alpha G(\zeta+x)+(1-\alpha)G(\zeta+x')}{\sqrt{(2\pi)^{\hat{n}\hat{T}}|\hat{\Sigma}|^\dagger}} e^{-\frac{1}{2}\zeta^\mathsf{T}\hat{\Sigma}^\dagger\zeta} d\zeta \\ &= \alpha\overline{G}(x) + (1-\alpha)\overline{G}(x'), \end{aligned}$$

which shows the convexity of $\overline{G}(\cdot)$. Furthermore, (29) is transformed into (36) by the fact that a chance constraint on a scalar Gaussian random variable $x \sim \mathcal{N}(\mu, \sigma^2)$ can be translated into a deterministic constraint, i.e., $\Pr(x < 0) < \delta$ if and only if $\mu > \sqrt{2\sigma^2}\mathrm{erf}^{-1}(1-2\delta)$; see [17]. ■

Proposition 1 shows that Problem 3 can be equivalently transformed into the deterministic convex optimization problem in (35). This deterministic representation indicates that a larger variance Σ of $\mathbf{d}$ in (5) makes the inequality constraint tighter. This is confirmed by the fact that $s_i(\hat{\Sigma}, \delta_i)$ in (36) is a monotonically increasing function with respect to the norm of Σ.

Note that $s_i(\hat{\Sigma}, \delta_i)$ is a function of the spatiotemporally aggregated variance $\hat{\Sigma}$, as defined in (24). To see the effect of this spatiotemporal aggregation by W more explicitly, we derive the bounds on its magnitude as follows:

Proposition 2: Consider Problem 3 and define $s_i(\hat{\Sigma}, \delta_i)$ as in (37). If $\delta_i \in (0, 0.5)$, then

$$0 < s_i(\hat{\Sigma}, \delta_i) \le \sqrt{\frac{2\nu\mathrm{tr}\,(\Sigma)}{\tau}}\, \|c_i\|\, \mathrm{erf}^{-1}(1-2\delta_i) \tag{38}$$

for each $i \in \{1, \dots, n_\mathrm{c}\}$.

Proof: From the definition of $\mathrm{erf}(\cdot)$ with $\delta_i \in (0, 0.5)$, the positivity of $s_i(\hat{\Sigma}, \delta_i)$ follows. Using the fact that

$$\mathrm{tr}(ABA^\mathsf{T}) \le \|A\|^2\mathrm{tr}(B)$$

for any $A \in \mathbb{R}^{m\times n}$ and positive semidefinite $B \in \mathbb{R}^{n\times n}$, we have

$$s_i(\Sigma, \delta_i) \le \sqrt{2\mathrm{tr}(\hat{\Sigma})}\, \|c_i\|\, \mathrm{erf}^{-1}(1-2\delta_i).$$

Furthermore, from $WW^\mathsf{T} = \frac{\nu}{\tau} I_{\hat{n}\hat{T}}$, it follows that

$$\mathrm{tr}(\hat{\Sigma}) \le \frac{\nu}{\tau}\mathrm{tr}(\Sigma).$$

Hence, (38) follows. ■

We explain the meaning of Proposition 2 by focusing on the inequality constraint on $\Delta\hat{\mathbf{X}}$ in (28). Note that the chance constraint on the ith element of $\Delta\hat{\mathbf{X}}$ is equivalently translated into (36) with $a_i = [0, e_i, -e_i]$, where e_i denotes the ith row of $I_{\hat{n}\hat{T}}$. Thus, we have $\|c_i\| = 1$. Because the scales of $\hat{\mathbf{X}}$, $\hat{\mathbf{D}}$ and $\hat{V}$ become necessarily larger owing to the summation by $\mathbf{1}_\nu^\mathsf{T}$ in (25), we evaluate $s_i(\hat{\Sigma}, \delta_i)$ by rescaling it as

$$0 < \frac{1}{\nu} s_i(\hat{\Sigma}, \delta_i) \le \sqrt{\frac{2\mathrm{tr}\,(\Sigma)}{\nu\tau}}\, \mathrm{erf}^{-1}(1-2\delta_i), \tag{39}$$

which implies that the inequality constraints in (36) can be relaxed by spatiotemporal aggregation. Thus, we can confirm that spatiotemporal aggregation works to expand the feasible solution space of Problem 3.

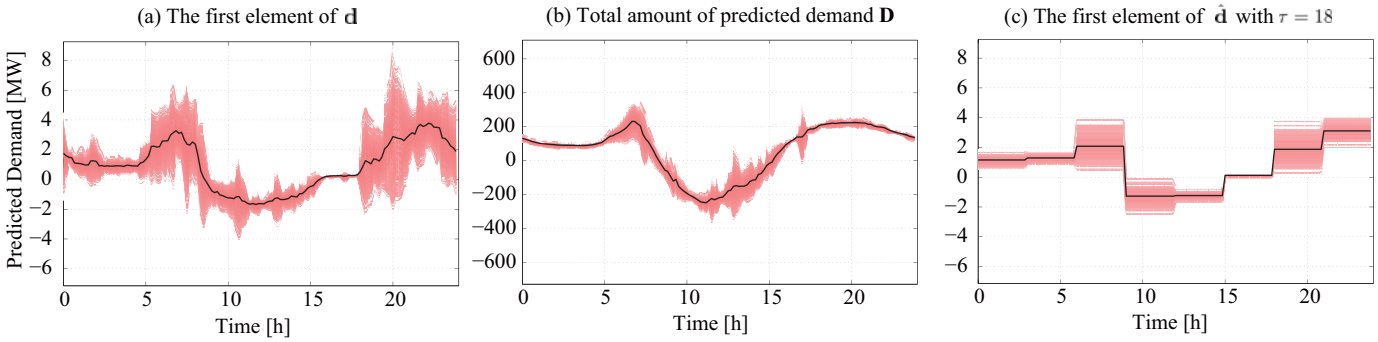

Fig. 2. Predicted demand and its spatiotemporal aggregation.

IV. Numerical Verification

In this section, we verify the efficiency of the proposed framework via a numerical experiment. We consider a power system managing 200 local areas, each of which includes 800 end users having PV power generators and storage batteries. In what follows, we regard a set of 800 end users as one consumer. This implies that the power system includes 200 consumers, i.e., $n = 200$.

As the predicted demand $\mathbf{d}$ in (5), we use the data of power consumption and PV power generation measured at houses in Ohta city, Japan. In particular, the mean value d is given as the average of five days in December 2007, and Σ is given as the sample covariance matrix of the five days of data. With $\kappa = 1/6$ [h] and $T = 144$ for (2), we plot the temporal sequence of the first element of $\mathbf{d}$, i.e., the temporal sequence of the demand of the first out of 200 consumers, every 10 minutes in Fig. 2(a), where the solid line depicts its mean value d, and the color density reflects the number of ratios for 1000 sample paths of $\mathbf{d}$. The mean value and the covariance matrix of demand for the other consumers are derived from the corresponding data; thus they are different from each other. In this section, the stochastic variables are depicted in the same manner as that in Fig. 2(a). On the basis of this demand prediction, we determine the day-ahead schedules of power generation and utility energy consumption requests to consumers.

A. Scheduling of Total Power Generation

We first find the optimal schedule of power generation, denoted by V^* in (12). For the cost function in (9), to evaluate the fuel cost of the generators, we give the first term by

(A3)

$$f(x) = 5.0x^2 + 2.2 \times 10^3 x.$$

Furthermore, to evaluate the deterioration cost of the storage batteries caused by discharging, we give the second term by

$$g(x) = \begin{cases} -4.6\gamma \times 10^4 x, & x < 0 \\ 0, & x \geq 0 \end{cases}$$

where $\gamma \in (0, 1]$ is a weighting parameter to be used below. The coefficients of $f(\cdot)$ are determined so as to approximate the fuel cost functions in [2] by a quadratic function [19], and the coefficients of $g(\cdot)$ are determined in compliance with the price and durability of a standard lithium ion battery [20]. In this formulation, $\gamma = 1$ corresponds to its current cost and durability; thus $\gamma < 1$ represents a future situation where the deterioration cost decreases in comparison with the current one.

Furthermore, the initial energy of a battery for every consumer, i.e., 800 end users, is given by 9.6 [MWh], i.e., $x_0 = 9.6\mathbf{1}_n$, which yields a total initial energy for all batteries of 1920 [MWh], i.e., $X(0) = 1920$. For the limitations on the amount of power generation, we give its upper and lower bounds as 480 [MW] and 0 [MW], i.e., $\mathcal{I}_4 = [0, 480]$ in (11).

Next, we fix the parameters of the chance constraints in (10). The total battery capacity is given by 3840 [MWh], which corresponds to the average capacity of storage batteries of 19.2 [MWh], and its lower bound is simply given by 0 [MWh], i.e., $\mathcal{I}_1 = [0, 3840]$. Similarly, the upper and lower bounds of the inverter capacity are given as 672 [MW] and -672 [MW], corresponding to the average capacity of the inverters of 3.36 [MW], i.e., $\mathcal{I}_2 = [-672, 672]$. Furthermore, the lower and upper bounds of the desired range of the battery energy given at the terminal time are supposed to be 40% and 60% of maximum battery energy, i.e., $\mathcal{I}_3 = [1536, 2304]$. For these constraints, we assign the violation rates as $\epsilon_1 = \epsilon_2 = 0.003$ and $\epsilon_3 = 0.35$. The values of ϵ_1 and ϵ_2 are given to comply with the three-sigma rule, which is often adopted in chance constrained optimization, and the value of ϵ_3 should be as small as possible to make the optimization problem feasible. Recall that the third chance constraint in (10) is given to approximately regulate the total battery energy at the termination time. Because the uncertainty of demand prediction is temporally integrated, i.e., pile up, over the whole day, we cannot make ϵ_3 small to comply with the three-sigma rule.

In Fig. 2(b), we show the temporal sequence of the spatially aggregated predicted demand, denoted by $\mathbf{D}$ in (6). Comparing Fig. 2(a) with Fig. 2(b), we can observe the smoothing effect, i.e., the accuracy of prediction is relatively improved by spatial aggregation. For this spatially aggregated predicted demand, varying the value of $\gamma \in (0, 1]$ in (9), we solve Problem 1 to find V^* in (12). The temporal sequence of V^* for each $\gamma \in \{1, 0.05, 0.01\}$ is plotted in Figs. 3(a)–(c) by the thick solid lines. From these figures, we see that the profiles of V^* tend to be flatter as the deterioration cost of storage batteries becomes lower.

B. Scheduling of Utility Energy Consumption Requests

Next, we find $\hat{v}^*$ in (22) by solving Problem 2. In this numerical experiment, we vary the degree of temporal resolu-

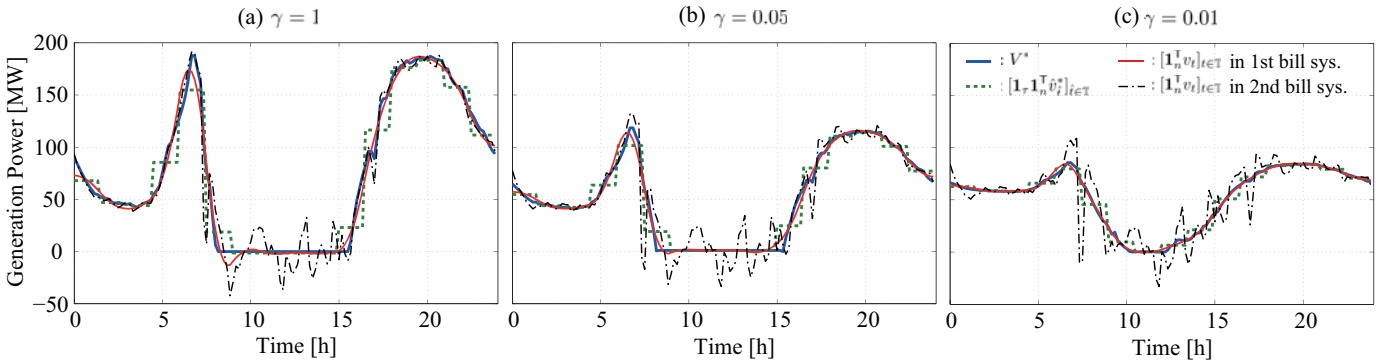

Fig. 3. Power generation schedules, total amounts of utility energy consumption requests, and total amounts of utility power consumption with $\tau = 9$.

tion as $\tau \in \{4, 9, 18\}$, which implies that the utility energy consumption requests to consumers are provided for each period $\hat{\kappa}$ of $2/3$, 1.5, and 3 [h]. In Fig. 2(c), we plot the temporal sequence of the first element of $\hat{\mathbf{d}}$ in (16) with $\tau = 18$, whose prediction accuracy is relatively improved compared with that in Fig. 2(a) owing to temporal aggregation.

The parameters in Problem 2 are given as follows. The upper and lower limits of utility energy consumption requests are given as 2.4 [MW] and -2.4 [MW], whose negativity represents that consumers are allowed to transfer some electric power to the others, i.e., $\hat{\mathcal{I}}_4 = [-2.4\mathbf{1}_n, 2.4\mathbf{1}_n]$ in (20). As for the chance constraints in (18), the intervals $\hat{\mathcal{I}}_i$ for $i \in \{1, 2, 3\}$ are given on the basis of the devision of $\mathcal{I}_i$ by $n = 200$, e.g., $\hat{\mathcal{I}}_1 = \frac{1}{200}[0, 3840\mathbf{1}_n]$. Furthermore, the violation rates are given as $\hat{\epsilon}_1 = \hat{\epsilon}_2 = 0.003$ and $\hat{\epsilon}_3 = 0.35$, which are the same values as those for total power generation scheduling.

Next, for each $\tau \in \{4, 9, 18\}$, we find the optimal schedule of requests, denoted by $\hat{v}^*$ in (22), as the solution of Problem 2. Then, it turns out that the optimization problem is infeasible when $\tau = 4$. To clarify the reason for this result, we plot the chance constraints of $\Delta\hat{\mathbf{x}}$ in (18) corresponding to the cases of $\tau \in \{4, 9, 18\}$ in Fig. 4, which are denoted by the thin solid lines, the thin dotted lines and the thick dotted lines, respectively. Note that the chance constraints on $\Delta\hat{\mathbf{x}}$ are equivalently translated into the deterministic constraints on $\Delta\hat{X}$ in (33) as

$$-\frac{672}{200}\mathbf{1}_{n\hat{T}} + s_{\mathcal{J}}(\Sigma, \hat{\epsilon}_2) \le \Delta\hat{X} \le \frac{672}{200}\mathbf{1}_{n\hat{T}} - s_{\mathcal{J}}(\Sigma, \hat{\epsilon}_2)$$

where $s_{\mathcal{J}}(\hat{\Sigma}, \hat{\epsilon}_2)$ denotes a vector composed of $s_i(\hat{\Sigma}, \hat{\epsilon}_2)$ compatible with $\Delta\hat{X}$. From this figure, we see that the upper and lower constraints for $\tau = 4$ overlap around 20 [h], i.e., the optimization is infeasible. That is, such a small degree of freedom cannot allow the idiosyncratic behavior of consumers. This result has some analogy to the conventional scheduling of generators subject to physical constraints such as ramping performance. In view of this, the use of signals with lower temporal resolution is expected to be one reasonable approach to such a scheduling problem with physical constraints.

For each $\gamma \in \{1, 0.05, 0.01\}$ with $\tau = 9$, the total amounts of optimal utility energy consumption requests, i.e., $[\mathbf{1}_\tau \mathbf{1}_n^\mathsf{T} \hat{v}_{\hat{t}}^*]_{\hat{t}\in\hat{\mathbb{T}}}$, are plotted in Figs. 3(a)–(c) by the thick dotted lines, where the temporal interpolation based on the zero-order hold is applied to draw them. From these figures, we see

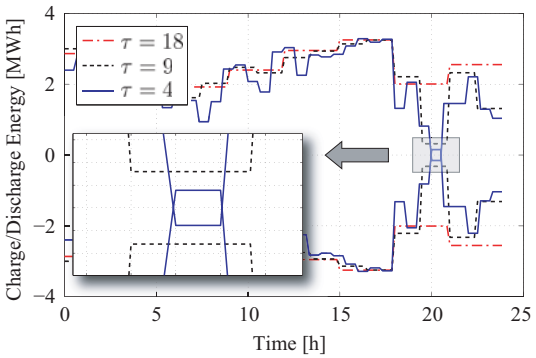

Fig. 4. Chance constraints with $\tau \in \{4, 9, 18\}$.

that the total amounts of resulting requests approximate the optimal total power generation schedules, i.e., V^* denoted by the thick solid lines. On the other hand, in the same manner, the total amounts of resulting requests with $\tau = 18$ are plotted in Figs. 5(a)–(c). Comparing these figures with Figs. 3(a)–(c), we see that the discrepancies between $[\mathbf{1}_\tau \mathbf{1}_n^\mathsf{T} \hat{v}_{\hat{t}}^*]_{\hat{t}\in\hat{\mathbb{T}}}$ and V^* become larger than those with $\tau = 9$, especially around the peak times of V^*. This difference is caused by the fact that the temporal resolution of the utility energy consumption requests is lower.

C. Management on the Day of Interest

In this subsection, we perform a simulation of the management on the day of interest, according to the resulting schedules of total power generation and utility energy consumption requests, denoted by V^* and $\hat{v}^*$, respectively. In the following, we regard the temporal sequence of the actual demand, i.e., d in (4), as one sample path of $\mathbf{d}$.

Through the management of the power system, we investigate what types of billing systems (or incentives) can make the the utility energy consumption requests reasonable in the sense that the total amount of actual utility power consumption is made closer to the optimal schedule of total power generation. Let

$$v = [v_t]_{t\in\mathbb{T}} \in \mathbb{R}^{nT}, \quad \Delta x = [x_{t+1} - x_t]_{t\in\mathbb{T}} \in \mathbb{R}^{nT}$$

denote the utility power consumption and battery charging power of the consumers, respectively, whose temporal sequences obey (4) with a sample path d. Then, we consider the cases where an independent system operator determines a

power bill charged to each consumer on the basis of either of the following billing systems:

$$F(v;x) = \begin{cases} F_1(v) + \frac{1}{100}F_2(v) \\ F_1(v) + \frac{1}{100}F_3(x) \end{cases} \tag{40}$$

where

$$\begin{aligned} F_1(v) &:= \left\| \left[\tfrac{1}{\tau} \left(v_{\tau\hat{t}} + \cdots + v_{\tau(\hat{t}+1)-1} \right) - \hat{v}^*_{\hat{t}} \right]_{\hat{t}\in\hat{\mathbb{T}}} \right\|^2 \\ F_2(v) &:= \left\| [v_{t+1} - v_t]_{t\in\mathbb{T}} \right\|^2, \\ F_3(x) &:= \left\| [\Delta x_{t+1} - \Delta x_t]_{t\in\mathbb{T}} \right\|^2. \end{aligned}$$

The meanings of F_1, F_2 and F_3 are explained as follows: The function F_1 penalizes the discrepancy between the actual utility energy consumption and its request. The functions F_2 and F_3 penalize the changing rates of utility power consumption and battery charging power, respectively. In this simulation, we suppose that a home energy management system implemented at each consumer's home controls the utility power consumption while minimizing the power bill determined by either the first or second billing system in (40). Note that penalization by F_1 is made to be dominant in both billing systems. Owing to this, the consumers follow the utility energy consumption requests principally while suppressing the changing rates of utility power consumption or battery charging power collaterally.

In this formulation, we calculate the total amount of actual utility power consumption, i.e., $[\mathbf{1}_n^\mathsf{T} v_t]_{t\in\mathbb{T}}$. When implementing the first billing system in (40), we obtain the temporal sequences of $[\mathbf{1}_n^\mathsf{T} v_t]_{t\in\mathbb{T}}$ for each $\gamma \in \{1, 0.05, 0.01\}$ as the thin solid lines in Figs. 3(a)–(c) and Figs. 5(a)–(c), which correspond to each $\tau \in \{9, 18\}$, respectively. From these results, we see that the sequences of $[\mathbf{1}_n^\mathsf{T} v_t]_{t\in\mathbb{T}}$ with $\tau = 9$ are close to those of V^* for all $\gamma \in \{1, 0.05, 0.01\}$. On the other hand, in the case of $\tau = 18$, the discrepancy is small only for $\gamma = 0.01$, which corresponds to a situation where the deterioration cost of the storage batteries becomes considerably low. The negative values of $[\mathbf{1}_n^\mathsf{T} v_t]_{t\in\mathbb{T}}$ can be regarded as the negative deviation from a base level of the total power generation or the total amount of power to be consumed on the supplier side.

Furthermore, we obtain $[\mathbf{1}_n^\mathsf{T} v_t]_{t\in\mathbb{T}}$ as the dashed-dotted lines in Figs. 3(a)–(c) and Figs. 5(a)–(c) when implementing the second billing system in (40), where a number of apparent spikes in the total utility power consumption occur. These spikes would originate from the fact that the effects of the steep fluctuations in PV power generation and the idiosyncratic behavior of consumers mostly appear as their utility power consumption because consumers tend to avoid penalization for their changing rate of battery charging power by F_3 in (40). From these results, we can conclude that the first billing system in (40) is generally better than the second one in the sense that the total amount of actual utility power consumption is made to be closer to the optimal schedule of total power generation.

Note that the discrepancy between the optimal schedule of total power generation and the total amount of actual utility power consumption, i.e., $V^* - [\mathbf{1}_n^\mathsf{T} v_t]_{t\in\mathbb{T}}$, can be regarded as the regulating capacity of spinning reserve generators required on the day of interest. From this numerical experiment, we can confirm that the regulating capacity of spinning reserve generators can be reduced by regulating the degree of freedom for utility power consumption with the implementation of a suitable billing (or incentive) system. A mathematical analysis and synthesis of billing systems would be meaningful future works to pursue.

V. Concluding Remarks

In this paper, we have proposed a novel framework to maintain the balance among the amounts of power generation, demand, and battery charging power under the supposition of large-scale penetration of PV power generators and storage batteries. The main features of our framework are summarized as follows:

- A load dispatching center provides utility energy consumption requests to individual consumers, which make battery charge cycles of consumers contribute to the supply-demand-storage balancing, via spatiotemporally multiresolutional modeling of power systems.
- On the basis of the idea that the small dispersion of quantities with regard to a large number of consumers is imperceptible to the supplier side owing to spatiotemporal aggregation, we determine the utility energy consumption requests with low temporal resolution, which not only ensures a degree of freedom for consumers with respect to utility power consumption but also relatively reduces the prediction uncertainty of PV power generation and power consumption.

The performance of our framework has been demonstrated via a numerical experiment, in which we have used the data of actual power consumption and PV power generation measured from houses in Ohta city, Japan. With this numerical experiment, we have demonstrated a trade-off relation in which the required regulating capacity of spinning reserve generators can be reduced by regulating the degree of freedom for utility power consumption, ensured for each consumer. On the other hand, it also turns out that the idiosyncratic behavior of consumers cannot be allowed if the degree of freedom is too small in comparison with the magnitude of the prediction uncertainty of power consumption and PV power generation.

The validity of our strategy for controlling the battery charging power on the consumer side is reliant on the *variety* of power consumption and PV power generation. In particular, from the law of large numbers, we can expect that the total amount of power consumption is close to its average over all consumers, which is relatively easy to predict, as long as the behavior of each consumer is sufficiently dispersed. Conversely, one possible concern would be raised by the *resonant* behavior of consumers due to synchronism of requesting periods for utility energy consumption requests, which can invoke unexpected peaks in the total power consumption. One remedy for this is to shift the timing of the requesting periods by dividing consumers into several groups. In fact, such a time-shift of requesting periods has the potential to improve the temporal resolution of the total number of utility energy

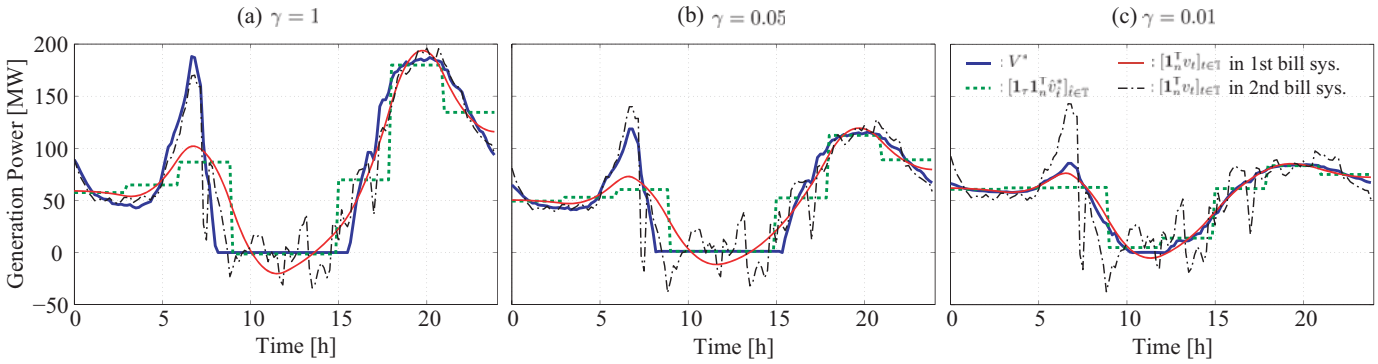

Fig. 5. Power generation schedules, total amounts of utility energy consumption requests, and total amounts of utility power consumption with $\tau = 18$.

consumption requests. The development of this time-shifting strategy is one future work to pursue. In addition, further consideration on detailed elements, e.g., the charge/discharge efficiency of storage batteries and the non-normal distribution of prediction errors, is meaningful to make our analysis more realistic. Such generalization would require more careful treatment for the switching of charge/discharge in translating a stochastic optimization problem to its deterministic representation. More specifically, in stochastic optimization, it is not straightforward to formulate the switching of variables for charge and discharge because a stochastic variable cannot be confined to a specific domain, such as the nonnegative orthant, in the almost sure sense. In view of this, the explicit consideration on the charge/discharge efficiency of storage batteries is a challenging task to work on. (A2)

List of Symbols

Preliminaries and numerical verification

t Time variable in original time scale
T Time length in original time scale
$\mathbb{T}$ Time set in original time scale
κ Unit of time step in original time scale
v Utility power consumption of consumers
d Net amount of demand of consumers
x Battery energy of consumers
$\mathbf{d}$ Predicted demand
Σ Covariance matrix for demand prediction

Scheduling of total power generation

V^* Optimal schedule of total power generation
V Total amount of power generation
$\mathbf{D}$ Total amount of predicted demand
$\mathbf{X}$ Total amount of battery energy
$\Delta\mathbf{X}$ Total amount of battery charging power
ϵ_i Violation rate for chance constraint
$\mathcal{I}_i$ Interval to constrain corresponding variable

Scheduling of utility energy consumption request

$\hat{t}$ Time variable in sparse time scale
$\hat{T}$ Time length in sparse time scale
$\hat{\mathbb{T}}$ Time set in sparse time scale
τ Degree of temporal resolution
$\hat{\kappa}$ Unit of time step in sparse time scale
$\hat{v}^*$ Optimal schedule of utility energy consumption request
$\hat{v}$ Request of utility energy consumption
$\hat{\mathbf{d}}$ Temporally aggregated predicted demand
$\hat{\mathbf{x}}$ Battery energy in sparse time scale
$\Delta\hat{\mathbf{x}}$ Battery charging power in sparse time scale
$\hat{\epsilon}_i$ Violation rate for chance constraint
$\hat{\mathcal{I}}_i$ Interval to constraint corresponding variable

Generalized scheduling

ν Degree of spatial resolution
$\hat{V}^*$ Optimal solution of generalized problem
$\hat{V}$ Decision variable of generalized problem
$\hat{\mathbf{D}}$ Spatiotemporally aggregated predicted demand
$\hat{\mathbf{X}}$ Spatiotemporally aggregated battery energy
$\Delta\hat{\mathbf{X}}$ Spatiotemporally aggregated battery charging power
$\hat{D}$ Mean of spatiotemporally aggregated predicted demand
$\hat{X}$ Mean of spatiotemporally aggregated battery energy
$\Delta\hat{X}$ Mean of spatiotemporally aggregated battery charging power
$\hat{\delta}_i$ Violation rate for chance constraint

Notation of Mathematics We denote the set of real numbers by $\mathbb{R}$, the n-dimensional unit matrix by I_n, the n-dimensional all-ones vector by $\mathbf{1}_n$, the trace of a matrix M by $\mathrm{tr}(M)$, the block diagonal matrix having n matrices M on its block diagonal by $\mathrm{diag}_n(M)$, the expectation of a stochastic variable x by $\mathbb{E}[x]$, the probability of an event A by $\Pr(A)$, and the normally distributed stochastic variable with mean $m \in \mathbb{R}^n$ and variance Σ by $x \sim \mathcal{N}(m, \Sigma)$. The error function is defined by $\mathrm{erf}(x) := \frac{2}{\sqrt{\pi}} \int_0^x e^{-t^2} dt$ and its inverse is denoted by $\mathrm{erf}^{-1}(x)$, satisfying $\mathrm{erf}^{-1}(\mathrm{erf}(x)) = x$. Finally, we use the notation of $[x_i]_{i\in\{1,\ldots,n\}} := [x_1^\mathsf{T}, \ldots, x_n^\mathsf{T}]^\mathsf{T}$ for vectors x_i.

References

[1] G8 Hokkaido Toyako Summit Leaders Declaration. Available at: http://www.mofa.go.jp/policy/economy/summit/2008/doc.
[2] T. Masuta and A. Yokoyama, "Supplementary load frequency control by use of a number of both electric vehicles and heat pump water heaters," *Smart Grid, IEEE Transactions on*, vol. 3, no. 3, pp. 1253–1262, 2012.
[3] M. Paulescu, E. Paulescu, P. Gravila, and V. Badescu, *Weather Modeling and Forecasting of PV Systems Operation*. Springer, 2012.
[4] M. Patel, *Wind and Solar Power Systems: Design, Analysis, and Operation, Second Edition*. Taylor & Francis, 2012.
[5] H. Ohtake, K. Shimose, F. J. Silva, T. Takashima, T. Oozeki, and Y. Yamada, "Accuracy of the solar irradiance forecasts of the japan meteorological agency mesoscale model for the Kanto region, Japan." *Solar Energy*, vol. 98, Part B, pp. 138–152, 2013.
[6] E. Wiemken, H. Beyer, W. Heydenreich, and K. Kiefer, "Power characteristics of PV ensembles: experiences from the combined power production of 100 grid connected PV systems distributed over the area of Germany," *Solar Energy*, vol. 70, no. 6, pp. 513–518, 2001.
[7] T. Oozeki, K. Otani, T. Takashima, Y. Hishikawa, G. Koshimizu, Y. Uchida, and K. Ogimoto, "An evaluation method for smoothing effect on photovoltaic systems dispersed in a large area," in *Proc. Photovoltaic Specialists Conference (PVSC), 2009 34th IEEE*, 2009, pp. 2250–2251.

[8] D. Bienstock, M. Chertkov, and S. Harnett, "Robust modeling of probabilistic uncertainty in smart grids: Data ambiguous chance constrained optimum power flow," in *Decision and Control (CDC), 2013 IEEE 52nd Annual Conference on*. IEEE, 2013, pp. 4335–4340.
[9] A. Sturt and G. Strbac, "Efficient stochastic scheduling for simulation of wind-integrated power systems," *Power Systems, IEEE Transactions on*, vol. 27, no. 1, pp. 323–334, 2012.
[10] P. Meibom, R. Barth, B. Hasche, H. Brand, C. Weber, and M. O'Malley, "Stochastic optimization model to study the operational impacts of high wind penetrations in Ireland," *Power Systems, IEEE Transactions on*, vol. 26, no. 3, pp. 1367–1379, 2011.
[11] M. Arnold and G. Andersson, "Model predictive control of energy storage including uncertain forecasts," in *Power Systems Computation Conference (PSCC), Stockholm, Sweden*, 2011.
[12] G. Di Bella, L. Giarrè, M. Ippolito, A. Jean-Marie, G. Neglia, and I. Tinnirello, "Modeling energy demand aggregators for residential consumers," in *Decision and Control (CDC), 2013 IEEE 52nd Annual Conference on*. IEEE, 2013, pp. 6280–6285.
[13] A. Nayyar, J. Taylor, A. Subramanian, K. Poolla, and P. Varaiya, "Aggregate flexibility of a collection of loads," in *Decision and Control (CDC), 2013 IEEE 52nd Annual Conference on*. IEEE, 2013, pp. 5600–5607.
[14] T. Sadamoto, I. Muto, T. Ishizaki, M. Koike, and J. Imura, "Power supply scheduling optimization from a viewpoint of spatio-temporal aggregation," *Proc. of the 19th IFAC World Congress, to appear*, 2014.
[15] A. Ben-Tal, L. El Ghaoui, and A. Nemirovski, *Robust optimization*. Princeton University Press, 2009.
[16] J. Zhu, *Optimization of Power System Operation*. Wiley, 2009.
[17] L. Blackmore, H. Li, and B. Williams, "A probabilistic approach to optimal robust path planning with obstacles," in *Proc. American Control Conference, 2006*. IEEE, 2006.
[18] W. Härdle and L. Simar, *Applied multivariate statistical analysis*. Springer, 2007, vol. 22007.
[19] G. F. Reid and L. Hasdorff, "Economic dispatch using quadratic programming," *Power Apparatus and Systems, IEEE Transactions on*, vol. 92, no. 6, pp. 2015–2023, 1973.
[20] Specification of lithium ion batteries. http://www.edisonpower.co.jp/_file/epups-ver14.pdf.

Tomonori Sadamoto was born in Chiba, Japan, in 1987. He received the B.E. and M.E., from Tokyo Institute of Technology, Tokyo, Japan, in 2009 and 2011, respectively. From 2011 through 2013, he was with Technology Research Center of Sumitomo Heavy Industries. Since April 2013, he has been a Ph.D student at the Department of Mechanical and Environmental Informatics, Graduate School of Information Science and Engineering, Tokyo Institute of Technology. He is a student member of IEEE.

Takayuki Ishizaki was born in Aichi, Japan, in 1985. He received the B.Sc., M.Sc., and Ph.D. degrees in engineering from Tokyo Institute of Technology, Tokyo, Japan, in 2008, 2009, and 2012, respectively.

He served as a Research Fellow of the Japan Society for the Promotion of Science from April 2011 to October 2012. From October to November 2011, he was a Visiting Student at Laboratoire Jean Kuntzmann, Université Joseph Fourier, Grenoble, France. From June to October 2012, he was a Visiting Researcher at School of Electrical Engineering, Royal Institute of Technology, Stockholm, Sweden. Since November 2012, he has been with the Department of Mechanical and Environmental Informatics, Graduate School of Information Science and Engineering, Tokyo Institute of Technology, where he is currently an Assistant Professor. His research interests include the development of model reduction and its applications.

Dr. Ishizaki is a member of IEEE, SICE, and ISCIE. He was named as a finalist of the 51st IEEE CDC Best Student-Paper Award.

Masakazu Koike was born in Nagano, Japan, in 1981. Since April 2013, he is currently a Ph.D. Researcher at Department of Mechanical and Environmental Informatics, Graduate School of Information Science and Engineering, Tokyo Institute of Technology. His research interests include the development of control theory for pneumatic isolation tables.

Dr. Koike is a member of IEEE, JSME, SICE, and ISCIE.

Yuzuru Ueda received the B.S. degree in physics from Shinshu University, Nagano, Japan, in 1995, and Ph.D. degree in engineering from the Tokyo University of Agriculture and Technology, Tokyo, Japan, in 2007. From 1995 to 2003, he was with Applied Materials Japan, Inc., Tokyo, as a Process Engineer of semiconductor wafer plasma processing. Since 2008, he has been an Assistant Professor with the Graduate School of Science and Engineering, Tokyo Institute of Technology. His research interests include photovoltaic systems, grid connection of the distributed generator, and solar energy.

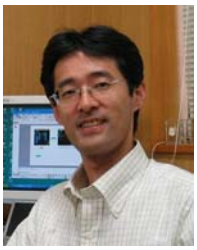

Jun-ichi Imura (M'93) was born in Gifu, Japan, in 1964. He received the M.S. degree in applied systems science and the Ph.D. degree in mechanical engineering from Kyoto University, Kyoto, Japan, in 1990 and 1995, respectively.

He served as a Research Associate in the Department of Mechanical Engineering, Kyoto University, from 1992 to 1996, and as an Associate Professor in the Division of Machine Design Engineering, Faculty of Engineering, Hiroshima University, from 1996 to 2001. From May 1998 to April 1999, he was a Visiting Researcher at the Faculty of Mathematical Sciences, University of Twente, Enschede, The Netherlands. Since 2001, he has been with the Department of Mechanical and Environmental Informatics, Graduate School of Information Science and Engineering, Tokyo Institute of Technology, Tokyo, Japan, where he is currently a Professor. His research interests include modeling, analysis, and synthesis of nonlinear systems, hybrid systems, and large-scale network systems with applications to biological systems, industrial process systems, and robot intelligence. He is an Associate Editor of Automatica (2009-), the Nonlinear Analysis: Hybrid Systems (2011-), and IEEE Trans. on Automatic Control (2014-).

Dr. Imura is a member of IEEE, SICE, ISCIE, IEICE, and The Robotics Society of Japan.